Trifluoperazine, an Antipsychotic Agent, Inhibits Cancer Stem Cell Growth and Overcomes Drug Resistance of Lung Cancer

Chi-Tai Yeh[1,2,3,4*], Alexander T. H. Wu[5,6*], Peter M.-H. Chang[7,8*], Kuan-Yu Chen[9*], Chia-Ning Yang[10], Shuenn-Chen Yang[11], Chao-Chi Ho[9], Chun-Chi Chen[11†], Yu-Lun Kuo[12], Pei-Ying Lee[13], Yu-Wen Liu[13], Chueh-Chuan Yen[7,14], Michael Hsiao[15], Pei-Jung Lu[16], Jin-Mei Lai[17], Liang-Shun Wang[1,18], Chih-Hsiung Wu[2], Jeng-Fong Chiou[6,19], Pan-Chyr Yang[9,11,20‡], and Chi-Ying F. Huang[8,13‡]

[1]Graduate Institute of Clinical Medicine, [3]Center of Excellence for Cancer Research, and [5]Ph.D. Program for Translational Medicine, College of Medical Science and Technology, Taipei Medical University, Taipei, Taiwan; [2]Department of Surgery, and [18]Division of Thoracic Surgery, Department of Surgery, Taipei Medical University-Shuang Ho Hospital, Taipei, Taiwan; [4]Graduate Institute of Medical Sciences, National Defense Medical Center, Taipei, Taiwan; [6]Translational Research Laboratory, Cancer Center, and [19]Department of Radiation Oncology, Taipei Medical University Hospital, Taipei, Taiwan [7]Division of Hematology and Oncology, Department of Medicine, Taipei Veterans General Hospital, Taipei, Taiwan; [8]Institute of Clinical Medicine, [13]Institute of Biopharmaceutical Sciences, and [14]Faculty of Medicine, National Yang-Ming University, Taipei, Taiwan; [9]Division of Pulmonary Medicine, Department of Internal Medicine, National Taiwan University Hospital and College of Medicine, Taipei, Taiwan; [10]Institute of Biotechnology, National University of Kaohsiung, Kaohsiung, Taiwan; [11]Institute of Biomedical Sciences and [15]Genomics Research Center, Academia Sinica, Taipei, Taiwan; [12]Department of Computer Science and Information Engineering, and [20]NTU Center for Genomic Medicine, College of Medicine, National Taiwan University, Taipei, Taiwan; [16]Institute of Clinical Medicine, National Cheng Kung University, Tainan, Taiwan; and [17]Department of Life Science, Fu Jen Catholic University, New Taipei City, Taiwan

***Rationale*: Cancer stem cell (CSC) theory has drawn much attention, with evidence supporting the contribution of stem cells to tumor initiation, relapse, and therapy resistance.**

***Objectives*: To screen drugs that target CSCs to improve the current treatment outcome and overcome drug resistance in patients with lung cancer.**

***Methods*: We used publicly available embryonic stem cell and CSC-associated gene signatures to query the Connectivity Map for potential drugs that can, at least in part, reverse the gene expression profile of CSCs. High scores were noted for several phenothiazine-like**

AT A GLANCE COMMENTARY

Scientific Knowledge on the Subject

Lung cancer is the leading cause of cancer death worldwide. Seventy percent of all patients with non–small cell lung cancer have inoperable disease and need systemic therapy. Resistance to chemotherapy or targeted therapy, such as epidermal growth factor receptor–tyrosine kinase inhibitor, is a major problem for systemic lung cancer treatment. Such resistance may be explained by cancer stem-like cell (CSC) theory. CSCs have been shown to possess stem cell characteristics, such as self-renewal, stress and drug resistance, and enhanced migration, all of which have been implicated in disease recurrence and distant metastasis. However, the optimal method of establishing a platform for screening drugs for CSCs remains to be explored.

What This Study Adds to the Field

Using a Connectivity Map dataset, this study identified a phenothiazine-like antipsychotic drug, trifluoperazine, which may reverse CSC-associated gene expression. Further *in vitro* and *in vivo* experiments validated its anti-CSC effects. Trifluoperazine in combination with either cisplatin or gefitinib had a synergistic cytotoxic effect on resistant lung cancer cells. This study demonstrated a novel platform for screening potential anti-CSC drugs, which may overcome drug resistance. By repurposing old drugs, which have a well-known safety profile, it may be possible to shorten the duration of drug development so that clinical trials can be conducted earlier.

(*Received in original form July 9, 2012; accepted in final form September 5, 2012*)

* These authors contributed equally to this work.

† Current address: CAS Key Laboratory of Pathogenic Microbiology and Immunology, Institute of Microbiology, Chinese Academy of Sciences, Beijing 100101, China.

‡ These authors contributed equally to this work.

Supported by grants from the National Science Council (NSC101-2325-B-010-011 and NSC100-2627-B-010-005 to C.-Y.F.H., NSC101-2325-B-038-005 and NSC100-2313-B-038-001-MY3 to C.-T.Y., NSC99-2628-B-038-010-MY3 to A.T.H.W., NSC101-2314-B-002-176 to K.-Y.C., and NSC101-2314-B-075-042 to P.M.-H.C.), and the Ministry of Education, Aim for the Top University Plan (National Yang Ming University), National Taiwan Normal University (100NTNU-D-06), and the Ministry of Economic Affairs (100-EC-17-A-17-S1-152) to C.-Y.F.H. This study was also supported by grants from the Center of Excellence for Cancer Research at Taipei Veterans General Hospital (DOH101-TD-C-111-007) to C.-Y.F.H. and at Taipei Medical University (DOH101-TD-C-111-008) to C.-T.Y.; and grants from Taipei Medical University (TMU 100-AE3-Y02 to A.T.H.W. and TMU100-AE3-Y04 and 101TMU-SHH-04 and to C.-T.Y.), Taipei Veterans General Hospital (V99B1-017), and the Taiwan Clinical Oncology Research Foundation to P.M.-H.C.

Author Contributions: C.-T.Y., conception and design, collection and assembly of data, data analysis and interpretation, manuscript writing; A.T.H.W., conception and design, collection and assembly of animal data, data analysis and interpretation, manuscript writing; P.M.-H.C., K.-Y.C., conception and design, data analysis and interpretation, manuscript writing; C.-N.Y., SAR analysis and interpretation, manuscript writing; S.-C.Y., C.-C.H., C.-C.C., generate cell lines; Y.-L.K., connectivity map analysis; P.-Y.L., Y.-W.L., P.-J.L., J.-M.L., L.-S.W., C.-H.W., J.-F.C., collection and assembly of data; C.-C.Y., conception and connectivity map analysis; M.H., animal study; P.-C.Y., data analysis and interpretation, manuscript writing, final approval of manuscript; C.-Y.F.H., conception and design, data analysis and interpretation, manuscript writing, final approval of manuscript.

Correspondence and requests for reprints should be addressed to Chi-Ying F. Huang, Ph.D., Institute of Biopharmaceutical Sciences, National Yang-Ming University, Taipei, Taiwan. E-mail: cyhuang5@ym.edu.tw

This article has an online supplement, which is accessible from this issue's table of contents at www.atsjournals.org

Am J Respir Crit Care Med Vol 186, Iss. 11, pp 1180–1188, Dec 1, 2012

Originally Published in Press as DOI: 10.1164/rccm.201207-1180OC on September 28, 2012
Internet address: www.atsjournals.org

antipsychotic drugs, including trifluoperazine. We then treated lung CSCs with different *EGFR* mutation status with trifluoperazine to examine its anti-CSC properties. Lung CSCs resistant to epidermal growth factor receptor–tyrosine kinase inhibitor or cisplatin were treated with trifluoperazine plus gefitinib or trifluoperazine plus cisplatin. Animal models were used for *in vivo* validation of the anti-CSC effect and synergistic effect of trifluoperazine with gefitinib.

***Measurements and Main Results*: We demonstrated that trifluoperazine inhibited CSC tumor spheroid formation and down-regulated the expression of CSC markers (CD44/CD133). Trifluoperazine inhibited Wnt/β-catenin signaling in gefitinib-resistant lung cancer spheroids. The combination of trifluoperazine with either gefitinib or cisplatin overcame drug resistance in lung CSCs. Trifluoperazine inhibited the tumor growth and enhanced the inhibitory activity of gefitinib in lung cancer metastatic and orthotopic CSC animal models.**

***Conclusions*: Using *in silico* drug screening by Connectivity Map followed by empirical validations, we repurposed an existing phenothiazine-like antipsychotic drug, trifluoperazine, as a potential anti-CSC agent that could overcome epidermal growth factor receptor–tyrosine kinase inhibitor and chemotherapy resistance.**

Keywords: trifluoperazine; lung cancer; cancer stem cell; gefitinib; connectivity map

Lung cancer is the leading cause of cancer deaths worldwide (1). Most patients with advanced-stage lung cancer receiving front-line chemotherapy experience disease progression (2). Resistance to chemotherapy and epidermal growth factor receptor–tyrosine kinase inhibitor (EGFR-TKI) is a major clinical problem. Thus, agents capable of overcoming drug resistance are urgently needed.

Recently, the cancer stem-like cell (CSC) hypothesis has drawn much attention. CSCs possess stem cell characteristics, including self-renewal, stress and drug resistance, and enhanced migration, which may contribute to tumor recurrence, metastasis, and chemoresistance (3–6). Putative lung CSCs were first identified as $CD133^+/Oct4^+/Nanog^+$ cells (7), and isolated in established non–small cell lung cancer (NSCLC) cell lines (8, 9). Lung CSCs may share functional features with lung progenitor cells, including the ability to actively exclude the dye Hoechst 33342, which defines them as side population cells in flow cytometric assays (10), and displays high aldehyde dehydrogenase (ALDH) activity (11). CSCs express high levels of ABCG2, a multidrug transporter, and demonstrate resistance to TKI treatment by modulating intracellular TKI concentrations (12).

Targeting CSCs among cancer cells by identifying distinct gene signatures may be critical in overcoming drug resistance. The consensus stemness signature in CSC-enriched samples was used to identify compounds that specifically target CSC-associated phenotypes (13). Wong and coworkers (14) used a higher-order and systems-level analysis to identify a differential gene signature between embryonic stem cells (ESCs) and adult tissue stem cells. They found that the ESC-like genes are also frequently up-regulated in aggressive human epithelial cancers. This ESC-like signature was strongly correlated with c-Myc activation (14). Kim and coworkers (15) further demonstrated three independent modules embedded in the ESC transcription programs, and the Myc module was found to be the most highly correlated with cancer cells. Using Gene Set Enrichment Analysis, the ESC-module used by Wong and coworkers was similar to the Myc module (15), raising the possibility that targeting these specific cancer-associated ESC-like gene signatures could result in the inhibition of CSCs.

Recently, efforts have been made to reevaluate old drugs with a view to determining their potential to inhibit CSCs as an alternative and relatively rapid strategy for overcoming drug resistance. Connectivity Map (CMap; http://www.broad.mit.edu/cmap/) (16) was developed to store expression profiles of diseases, genes, and chemicals and to provide a query interface for making inferences based on the query and the internal profiles. We used established ESC-like gene signatures (14) combined with CMap analysis (16) to search for drugs with the potential to convert ESC-like gene signatures to adult stem cell signatures. One of the top-ranked candidates, trifluoperazine, was examined for its effects on lung cancer cells with different EGFR status *in vitro* and *in vivo* with gefitnib-resistant CSCs mouse models.

METHODS

Generation of a Stable Dual Reporter–expressing Lung Cancer Cell Line

The dual optical reporter system L2G fusion construct (firefly luciferase 2 and eGFP) was a generous gift from Dr. Gambhir, Stanford University. Stable L2G-expressing CL97 cells were generated accordingly. Briefly, CL97 cells with stable integration of the L2G reporter were generated by lentiviral-mediated gene transfer. 293FT cells were transfected with the lentiviral vector L2G, the packaging plasmid pCMVΔ8.74, and the envelope plasmid pMD2.G (17). The target CL97 cells were infected with the viral particles and selected using Zeocin. CL97 cells carrying the L2G reporter system (CL97-L2G) were obtained and expanded for further experiments.

Evaluation of Trifluoperazine's Anti-CSC Effects Using Noninvasive Bioluminescent Imaging

NOD/SCID mice were purchased from National Taiwan University and maintained in compliance with the institutional policy. All animal procedures were approved by the Institutional Animal Care and Use Committee at Taipei Medical University.

For bulk lung tumor model, CL97-L2G cells were intravenously administered into the animals by tail vein at a concentration of 1×10^6 cells/100 μl phosphate-buffered saline. One week post tumor injection, different treatment regimens were started. Four regimens were performed: trifluoperazine (5 mg/kg/day); gefitinib (150 mg/kd/day, oral gavage); and a combination of trifluoperazine (5 mg/kg/day intraperitoneal injection) + gefitinib (100 mg/kg/day, oral gavage) for a period of 4 weeks.

To examine the preventive and anti-CSC effects of trifluoperazine, CL97-L2G spheroids were pretreated with trifluoperazine (5 μM, $<IC_{50}$, overnight); resuspended from their spheroid form; and orthotopically injected into the lungs of NOD/SCID mice (1×10^4 cells/50 μl matrigel/inoculation). The animals did not receive further treatment for the span of the experiment. CL97-L2G–bearing mice (bulk lung tumor and CSC models) were imaged weekly using the IVIS 200 system (Caliper Life Sciences, Waltham, MA). Data are expressed as fold change in total photon flux/initial total photon flux and were analyzed using Living Image 1.0 software (Caliper Life Sciences). Mice were humanely killed at the end of experiments and lung tumor biopsies were obtained for further analysis.

Additional study methods, including MTT (3-[4,5-dimethylthiazol-2-yl]-2,5-diphenyltetrazolium bromide) assay, Western blot, cell culture, chemicals, clonogenic assay, Aldefluor assay, soft agar assay, tumor spheroid assay, and reporter assay, are described in the online supplement.

RESULTS

In Silico Drug Screening Revealed that Phenothiazine-like Antipsychotics Might Reverse ESC or CSC Gene Expression

Using an ESC gene signature (by comparing ESC gene expression and adult stem cell gene expression) as an input to query CMap, a total of 77 drugs with the potential to reverse ESC-like gene expression to adult stem cell gene expression were identified (Table 1) (with negative enrichment scores; $P < 0.05$). Seven drugs were phenothiazine-like antipsychotics (Table 1, *see* Table E1 in the online supplement). Further analysis using an additional ESC

signature and two CSC signatures (Table 1, *see* Tables E2–E4) indicated that these antipsychotic drugs might act as anti-CSC agents.

Next, we isolated CSC-like cells from the CL141 cell line using side population technique to examine the potential anti-CSC effects of these antipsychotics. Table 1 summarizes the results from the MTT (3-[4,5-dimethylthiazol-2-yl]-2,5-diphenyltetrazolium bromide), side population, and clonogenic assays. Four of the antipsychotics (trifluoperazine, thioridazine, chlorpromazine, and perphenazine) reduced the percentages (>50%) of side population cells among the CL141 cells (Table 1). To further analyze other antipsychotic drugs, we examined an additional 16 phenothiazine-like drugs and the results showed that trifluprom azine and promazine could reduce the percentages (>50%) of side population cells among the CL141 cells (*see* Table E5). Of the six effective antipsychotic drugs (Figure 1A), we chose to characterize the top-ranked drug, trifluoperazine, in the following experiments.

Trifluoperazine Inhibited Proliferation and Induced Apoptosis of Gefitinib-Resistant NSCLC Cells

We hypothesized that trifluoperazine would inhibit tumor growth and overcome drug resistance by exerting anti-CSC effects. In addition to the commonly used cell lines (A549 and H1975), we also established several cell lines including CL83, CL141, CL152, CL25, and CL97 cell lines, which were isolated from the pleural effusion of patients with NSCLC at the National Taiwan University Hospital. The investigation was approved by the Institutional Review Board of the National Taiwan University Hospital. Informed consent was obtained before pleural effusion was collected. A summary of the main features of these cell lines, including their histologic and mutational characteristics, and whether they have intrinsic or acquired resistance to EGFR-TKIs, is provided in Table 2. We demonstrated that trifluoperazine dose-dependently inhibited NSCLC cell growth, and the respective IC_{50} values (48-h incubation) for CL83, CL141, CL152, CL25, CL97, and H1975 were 14, 8.5, 12, 13, 7.2, and 15 μM, respectively (Table 2, *see* Figure E1).

Among these cell lines, we chose CL141, an adenocarcinoma with wild-type *EGFR* status that shows resistance to gefitinib, as a representative target cell line for apoptosis analysis. annexin V/PI staining was performed after treatment with different dosages of trifluoperazine. Early and late apoptotic cells were counted. After 48 hours, trifluoperazine-treated CL141 cells exhibited a dose-dependent increase in annexin V–positive cells compared with the control cells (Figure 1B). The results indicated that trifluoperazine inhibited the proliferation of and induced apoptosis of gefitinib-resistant NSCLC cells.

Trifluoperazine Reduced the Percentage of and Induced Apoptosis of Lung CSCs

We selected gefitnib-resistant cell lines CL83, CL141, CL152 (with wild-type *EGFR*), and CL97 (harboring *EGFR*-G719A+T790M mutations) and isolated their CSCs using side-population method (1.54%, 2.13%, 1.95%, and 1.9% of the side population cells, respectively). After treatment with 5 μM trifluoperazine, the percentage of side population cells significantly decreased (Figure 1C).

For further clarification, we examined if trifluoperazine treatment could deplete the percentage of the cells with ALDH expression, an established marker for hematopoietic and NSCLC CSCs. CL141 (adenocarcinoma) and CL152 (squamous cell carcinoma) were selected as representative target NSCLC cell lines. Trifluoperazine treatment decreased the $ALDH^+$ CL141 cell population from 4.31% to 0.84% and from 3.73% to 1.08% in CL152 cells (Figure 1D).

To investigate the apoptotic-associated signal transduction in lung CSC after trifluoperazine treatment, CL97 (adenocarcinoma with *EGFR*-T790M–acquired resistance mutation) was selected as a target cell line. After trifluoperazine treatment of CL97 cancer spheroids, Bax, Bak, cleaved PARP, caspase-3, and caspase-9 was increased dose-dependently, whereas antiapoptotic Bcl-2, XIAP, and Mcl-1 were decreased (Figure 1E).

Trifluoperazine Inhibited the Clonogenicity and Stemness-associated Markers of Lung CSCs

Three different gefitinib-resistant lung CSCs, including CL141 (wild-type *EGFR*), CL83 (wild-type *EGFR*), and CL97 (*EGFR*-G719A+T790M acquired resistance mutation) were treated with trifluoperazine to examine its effects on tumor spheroid formation. Trifluoperazine dose-dependently decreased the size and number in all spheroids (Figures 2A–2C). The mean colony formation of CL141 spheroids on soft agar decreased after 12 days of treatment with either 5 or 10 μM trifluoperazine (Figure 2C) (mean colony number, control, 125; 5 μM, 45; 10 μM, 5). CL141 and CL97 spheroids were treated with increasing dosages of trifluoperazine (0, 2.5, 5, and 10 μM) for 48 hours. Two established lung CSC markers, CD44 and CD133, were dose-dependently down-regulated by trifluoperazine as measured by Western blotting and immunochemical staining (Figures 2D and 2E).

To explore the molecular mechanisms mediated by trifluoperazine, CL97 spheroids were treated with trifluoperazine and analyzed by Western blots. Wnt/β-catenin signaling downstream targets, cyclin D1 and c-Myc, and c-Met were decreased by

TABLE 1. PHENOTHIAZINE-LIKE ANTIPSYCHOTICS APPEAR FREQUENTLY BY QUERYING THE CONNECTIVITY MAP USING EMBRYONIC STEM CELL OR CANCER STEM CELL–LIKE SIGNATURES FOR POTENTIAL ANTICANCER STEM CELL DRUGS

	Rank						
Drug Name	Wong and Coworkers	Shats and Coworkers	Suvà and Coworkers	Ramalho-Santos and Coworkers	MTT Assay (IC_{50}) (μM)	Clonogenic Assay (IC_{50}) (μM)	Reduced Side Population
Trifluoperazine	1	5	47	38	>10	1.25–2.5	Yes
Prochlorperazine	2	9	—	—	>10	5–10	No
Thioridazine	3	13	11	—	>10	2.5–5	Yes
Chlorpromazine	17	—	—	—	5–10	2.5–5	Yes
Fluphenazine	21	43	—	—	>10	ND	No
Acepromazine	60	—	—	—	>10	1–2.5	No
Promethazine	75	—	—	—	>10	5–10	No
Perphenazine	—	37	—	—	>10	5–10	Yes
Triflupromazine	—	—	—	—	>10	ND	Yes
Promazine	—	—	—	—	>10	ND	Yes

Definition of abbreviations: MTT = 3-(4,5-dimethylthiazol-2-yl)-2,5-diphenyltetrazolium bromide; ND = not determined.
MTT and clonogenic assays were performed for A549 cells, whereas the side population data were from experiments conducted on CL141 cells.

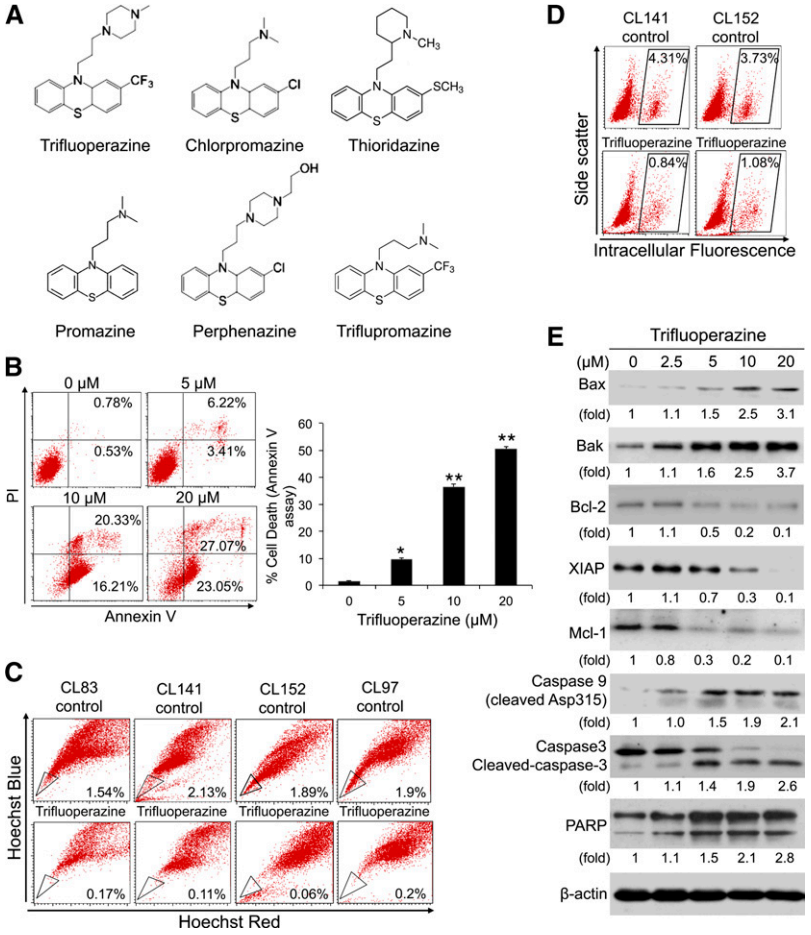

Figure 1. Trifluoperazine reduces the percentage of non–small cell lung cancer stem-like cells and induces apoptosis. (*A*) The structure of six antipsychotic drugs with the ability to reduce the percentages (>50%) of side population cells in the A549 cells. (*B*) The CL141 cell line was incubated with dimethyl sulfoxide or the indicated concentrations of trifluoperazine for 48 hours. The numbers indicate the percentages of total cells in the corresponding quadrant. The *bottom right quadrant* shows the early apoptotic cells, and the *top right quadrant* shows late apoptotic cells. All values are the average of triplicate experiments with the SD indicated by the error bars. (*C*) The cancer stem-like side population was significantly decreased by trifluoperazine (5 μM), from 2.13% to 0.11% in CL141 cells and from 1.89% to 0.06% in CL152 cells, as determined by side population assay. (*D*) The aldehyde dehydrogenase–positive subpopulation of cancer stem-like cells was also reduced by trifluoperazine (5 μM) from 4.31% to 0.84% in CL141 cells and in CL152 cells from 3.73% to 1.08%. (*E*) Trifluoperazine dose-dependently activated apoptotic signaling in CL97 spheroids, including Bax, Bak, cleaved PARP, caspase-3, and caspase-9, whereas the antiapoptotic proteins Bcl-2, XIAP, and Mcl-1 were downregulated.

trifluoperazine (Figure 2F). Additionally, trifluoperazine (at low concentration, 2.5 μM) inhibited TCF-mediated transcription in CL141 spheroids disrupted spheroid formation (Figure 2G).

Trifluoperazine Synergistically Inhibits Lung CSCs *In Vitro* while Combined with Cisplatin or Gefitinib

We selected three gefitinib-resistant NSCLC cell lines (CL141 [wild-type *EGFR*]; CL83 [wild-type *EGFR*]; and CL97 [*EGFR*-G719A+T790M acquired resistant mutation]) to determine if trifluoperazine could sensitize these cells toward chemotherapeutic agents. While treating with 10 μM of cisplatin for 24 hours, all CL141, CL83, and CL97 spheroids showed a significantly higher IC_{50} (Figure 3A) than their parental cells. Under the same condition, all spheroids showed higher viability and a lower caspase-3 activity as compared with their parental cells (Figures 3B and 3C).

Next, we examined whether trifluoperazine could enhance the cytotoxic effects of cisplatin or gefitinib. The combined trifluoperazine and cisplatin treatment provided a significantly higher cytotoxic effect in CL83 and CL141 spheroids than either trifluoperazine or cisplatin treatment alone (Figure 3D).

Assessment of the combinatorial activity of trifluoperazine and gefitinib was performed using the isobolographic method (18). Values below the line are synergistic, those close to the line are additive, and those above the line antagonistic. The synergistic activity of both agents was demonstrated from the normalized isobolograms obtained from the EGFR wild-type cells (CL141); EGFR-G719A+T790M mutation cells (CL97); and EGFR-exon 19 deletion cells (CL25) (Figure 3E). The enhanced cytotoxicity was also observed in all CL141, CL97, and CL25 spheroids. To investigate the effect of trifluoperazine on gefitinib therapy, CL25 (EGFR-TKI sensitive cell line) spheroids growth inhibition assay was performed as a positive control. CL25 spheroids were exposed to individual agents or a combination of trifluoperazine with gefitinib, and CL141 and CL97 cell lines (Figure 3F). Gefitnib alone effectively suppressed the spheroid formation in CL25 but significantly less in CL141 and CL97 cells. The combination of trifluoperazine and gefitnib significantly suppressed the spheroid formation of CL141 and CL97. These observations indicated that the addition of trifluoperazine sensitized gefitinib-resistant lung cancer cells. In addition, the percentage of $ALDH^+$ CL141 cells was moderately decreased at 10 μM of trifluoperazine. However, an enhanced inhibitory effect was observed when trifluoperazine was combined with 5 μM of gefitinib (Figure 3G). A similar enhanced inhibition on CL141 spheroid formation was observed (Figure 3H).

Trifluoperazine Treatment Suppressed Tumorigenesis of Gefitinib-Resistant CL97-L2G in Mouse Lung Cancer Models

NOD/SCID mice bearing gefitinib-resistant CL97-L2G (G719A+T790M acquired resistance mutation) cells were used to evaluate the antitumor effects of trifluoperazine. First, CL97 bulk tumor cells were injected intravenously into the tail vein of NOD/SCID mice that subsequently received vehicle with trifluoperazine alone (5 mg/kg/day, intraperitoneally), gefitinib alone (150 mg/kg/day, oral gavage), or a combination of trifluoperazine (5 mg/kg/day, intraperitoneally) and gefitinib (100 mg/kg/day, oral gavage) treatment (19, 20). Comparatively, mice that received trifluoperazine alone showed significantly lower tumor burden than those that received vehicle and gefitinib alone (Figure 4A).

TABLE 2. THE CLINICAL CHARACTERISTICS, GENE MUTATIONS, AND RESPONSES TO EGFR-TKI AND TRIFLUOPERAZINE FOR THE NON–SMALL CELL LUNG CANCER CELL LINES IN THIS STUDY

Cell Line	Sex	Histology	Clinical Information	EGFR Mutation Status	PTEN Mutation Status	p53 Mutation Status	KRAS Mutation Status	Resistance to EGFR-TKI	IC_{50} for Gefitinib	IC_{50} for Trifluoperazine
CL83	Male	Adenocarcinoma	Collected on the 16th day after gefitinib treatment, disease progression	WT	Normal	ND	WT	Intrinsic resistance	>10 μM	14 μM
CL141	Male	Adenocarcinoma	Collected while chemonaive	WT	Loss	R248W	WT	Intrinsic resistance	>10 μM	8.5 μM
CL152	Male	Squamous cell carcinoma	Collected while chemonaive	WT	Loss	R248W	WT	Intrinsic resistance	>10 μM	12 μM
CL25	Male	Adenocarcinoma	Collected before erlotinib treatment, partial response	Exon 19 deletion	Normal	C135Y	WT	Sensitive	50 nM	13 μM
CL97	Male	Adenocarcinoma	Collected after erlotinib and several cycles of chemotherapy, response to erlotinib use: disease progression	G719A/T790M	Normal	R273H	WT	Acquired resistance	>10 μM	7.2 μM
H1975	Female	Adenocarcinoma	Established in July 1988 from a nonsmoker	L858R/T790M	Normal	WT	WT	Intrinsic resistance	>10 μM	15 μM
A549	Male	Adenocarcinoma	Initiated in 1972 by Giard and coworkers through explant culture of lung carcinomatous tissue from a 58-yr-old white man	WT	Normal	WT	G12S	Intrinsic resistance	>10 μM	>10 μM

Definition of abbreviations: EGFR-TKI = epidermal growth factor receptor-tyrosine kinase inhibitor; ND = not determined; WT = wild-type.
The clinical information of H1975 and A549 was obtained from ATCC.

As expected, gefitinib-treated mice demonstrated a similar level of tumor burden as the vehicle control group. Mice that received the gefitinib-trifluoperazine combined treatment exhibited the lowest tumor burden. Tumor burden was measured and quantified based on the fold change in bioluminescence intensity.

In the prevention experiment, CL97-L2G cells were pretreated with vehicle or trifluoperazine (5 μM, $<IC_{50}$) and orthotopically implanted into NOD/SCID mice. Mice that received the trifluoperazine-pretreated CL97-L2G cells exhibited delayed and significantly reduced *in situ* tumor growth compared with vehicle-treated control mice (Figure 4B). To explore the molecular mechanisms mediated by trifluoperazine, total protein lysates were harvested from tumor samples. The expression level of stemness molecules including c-Myc and β-catenin was found to be decreased. Cyclin D1 expression was also suppressed by trifluoperazine and the combined treatment, whereas the activated form of caspase-3 was increased by trifluoperazine and the combined treatment (Figure 4C). Gefitinib treatment did not significantly influence the expression level of either c-Myc or β-catenin.

DISCUSSION

Our study demonstrates that trifluoperazine can be a potentially anti-CSC agent for NSCLC, as evidenced by its ability to suppress tumor spheroid formation and down-regulate Wnt/β-catenin signaling. More importantly, when combined with gefitinib or cisplatin, trifluoperazine was able to enhance treatment response and overcome drug resistance. Thus, we have demonstrated the feasibility of using CMap in combination with gene signatures for drug repurposing to target lung CSCs.

The availability of CMap offers an alternative tool in the drug discovery arena, and the use of this tool could promote Food and Drug Administration approval of old drugs for unmet clinical needs. The contributions of CSCs in tumor initiation, distant metastasis, drug resistance acquisition, and disease recurrence have been shown, and have recently gained recognition as hallmarks of cancer development (21). Therefore, targeting CSCs might provide a new treatment strategy for patients with drug resistance. To accelerate clinical use, possibly through drug repurposing, we focused on previously established antipsychotic drugs, specifically trifluoperazine.

Currently available conventional and targeted therapeutic agents eliminate the bulk of the tumor mass, but not CSCs (22). Thus, the identification and development of CSC-targeting agents is urgent. However, the drug development and approval process is uncertain, time-consuming, and expensive. To circumvent these obstacles and demonstrate proof-of-concept, we used a CMap dataset (16) in combination with gene expression array data of ESCs, CSCs, and adult stem cells to identify available clinical drugs with the potential to reverse CSC signatures. The rationale for using these datasets was that CSCs share a high degree of genetic similarities with ESCs, particularly the "Core" stemness gene signatures (23, 24). It is suspected that deregulation of these stemness genes and their products contributes to the development of CSCs. In particular, c-Myc and its associated genes were identified as a major molecular link between ESCs and CSCs (14, 15). In addition to the signature developed by Wong and coworkers (14), another ESC-like signature established by Ramalho-Santos and coworkers (25) was created using mouse embryonic, neural, and hematopoietic stem cells to define a genetic program for stem cells. Two additional CSC-associated signatures were used in the present study. One was established by Shats and coworkers (13), who determined the gene profiles of multiple cancer cell lines with differential stem-like characteristics, such as basal gene expression of breast cancer cells or $CD133^+$ versus glioma cells. The other dataset was from Suvà and coworkers (26), who treated primary gliospheroids with DZNep to impair their self-renewal ability. Using these gene expression profiles, we analyzed and highlighted the reversal of the ESC-CSC expression profiles by phenothiazines (*see* Tables E1–E4).

Among these phenothiazines, thioridazine has recently been shown to differentially inhibit leukemia stem cells compared with its effect on normal stem cells (27). In this study, we identified trifluoperazine using CMap analysis and determined that, as a candidate antilung CSC agent, it may be superior to thioridazine (Table 1). Because targeting CSCs focuses on inhibiting self-renewal ability rather than causing toxicity, these drugs are potentially less toxic than conventional chemotherapeutic

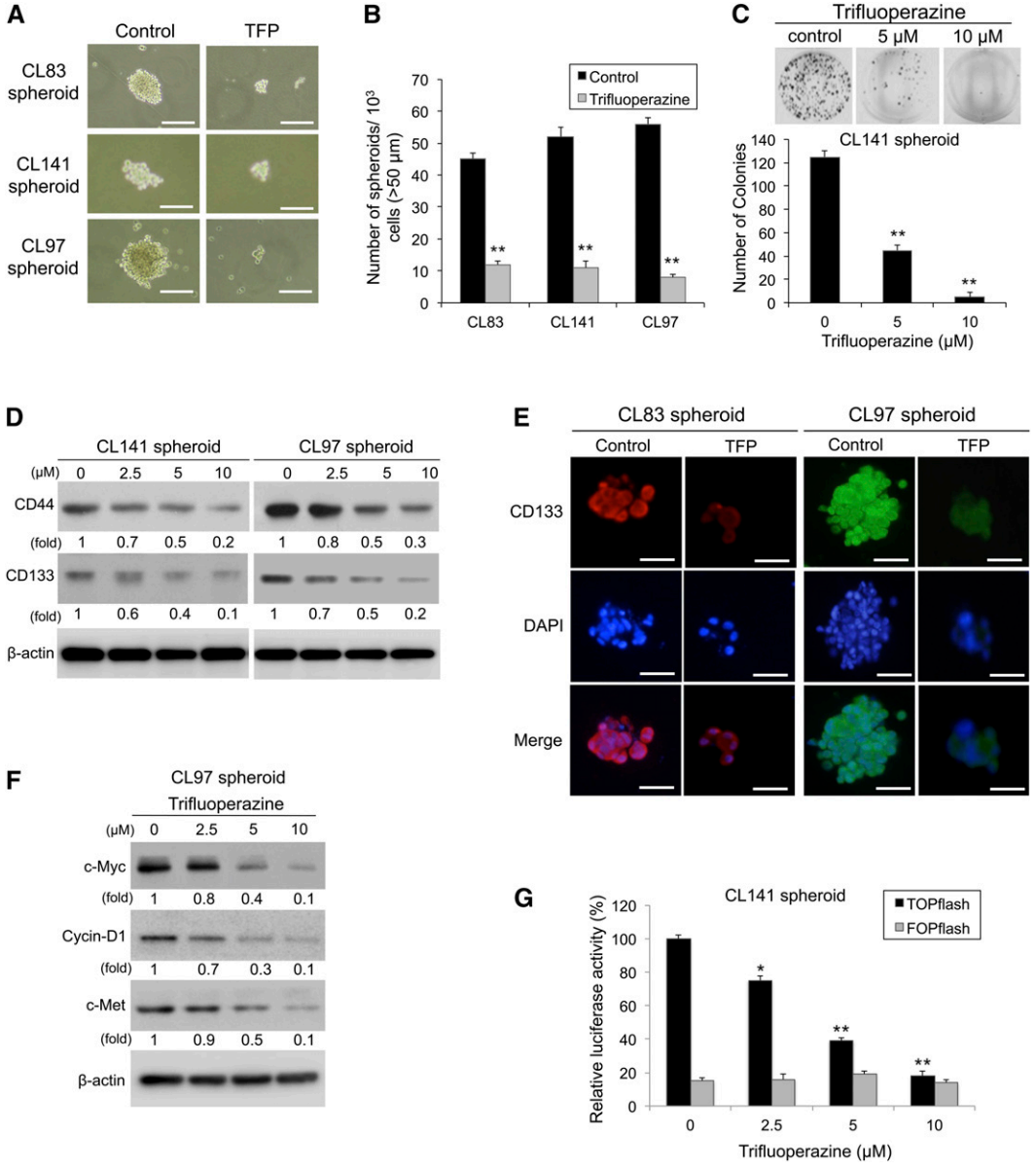

Figure 2. Trifluoperazine (TFP) inhibits the capacity of lung cancer spheroid self-renewal. (*A* and *B*) Treatment of TFP for 48 hours results in decreases of the size (*A*) and the number (*B*) of CL83, CL141, and CL97 spheroids, scale bar 50 μm. (*C*) CL141 cancer spheroids were seeded in six-well plates. Two weeks later, colonies containing more than 50 cells were counted by phase microscopy. The numbers of colonies in the control group was set at 100%, and the numbers of colonies present in the TFP-treated groups were calculated. (*D*) CL141 and CL97 cancer spheroids were treated with different doses of TFP for 48 hours. Expression of CD44 and CD133 was evaluated by Western blot analysis, and β-actin served as an internal control. (*E*) Various spheroids were immunostained for CD133 and nuclei counterstaining (DAPI) at 48 hours after TFP treatment as indicated. Photomicrographs were taken at ×40 magnification. (*F*) CL97 spheroids were treated with TFP at various concentrations for 48 hours. Cells were lysed for Western blot analysis by using antibodies specific to c-Myc, cyclin D1, and c-Met. (*G*) TCF/LEF transcription after treatment of CL141 cancer spheroids with different concentrations of TFP for 24 hours. Cells were lysed, and the TOPflash and FOPflash activities were recorded in a luminometer.

drugs, as reflected by their relatively higher than anticipated IC_{50} values (Table 1).

We isolated $CD44^+/CD133^+$ lung spheroids and demonstrated that trifluoperazine possesses anti-CSC properties, as evidenced by suppression of stemness-associated expression, such as CD133, c-Myc, and β-catenin, while modulating apoptotic factors, including Bax, Bad, Bcl-2, and caspases. It is noteworthy that the Wnt/β-catenin signaling axis has been implicated in the development and maintenance of CSCs in different tumor types (28). For instance, Wnt3a overexpression activated CSCs and induced metastasis by LEF1 and HOXB9 (29); furthermore, mutations in Wnt/β-catenin pathway components have been suggested as primary causes of lung tumorigenesis (25, 30). Notably, the expression level of c-Myc, a key molecular link between ESCs and cancer cells (14), was suppressed by trifluoperazine treatment. Although the exact mechanism of action mediated by trifluoperazine remains unclear, it has been shown that trifluoperazine may block dopamine D_1 and D_2 receptors in the mesocortical and mesolimbic pathways (31) in the treatment of schizophrenia (32). At low dosages, trifluoperazine functions as a calmodulin antagonist that blocks Ca^{2+}-calmodulin–dependent cellular events (33, 34). As a calmodulin antagonist, trifluoperazine inhibits cell proliferation and invasion, and induces apoptosis in several types of cancer cells (35–37). Trifluoperazine has also been shown to block the function of P-glycoprotein by modification of the membrane structure around P-glycoprotein or by direct interaction with P-glycoprotein (38). Notably, trifluoperazine has been shown to sensitize multidrug resistance–positive cells to chemotherapeutic agents (39, 40), which supports the finding of the present study (i.e., trifluoperazine sensitized gefitinib-resistant CL97 cells). Thus, trifluoperazine was further shown to possess antilung CSC characteristics.

The CSC hypothesis has emerged as an important milestone in the understanding of drug resistance and disease recurrence (41). Based on their characteristics, targeting and eradicating CSCs represents a potential strategy for significantly improving clinical outcome or for possibly achieving complete remission. Because we established that trifluoperazine can disrupt major signaling pathways that are activated in CSCs and cancer cells, we investigated whether trifluoperazine could enhance the activity of

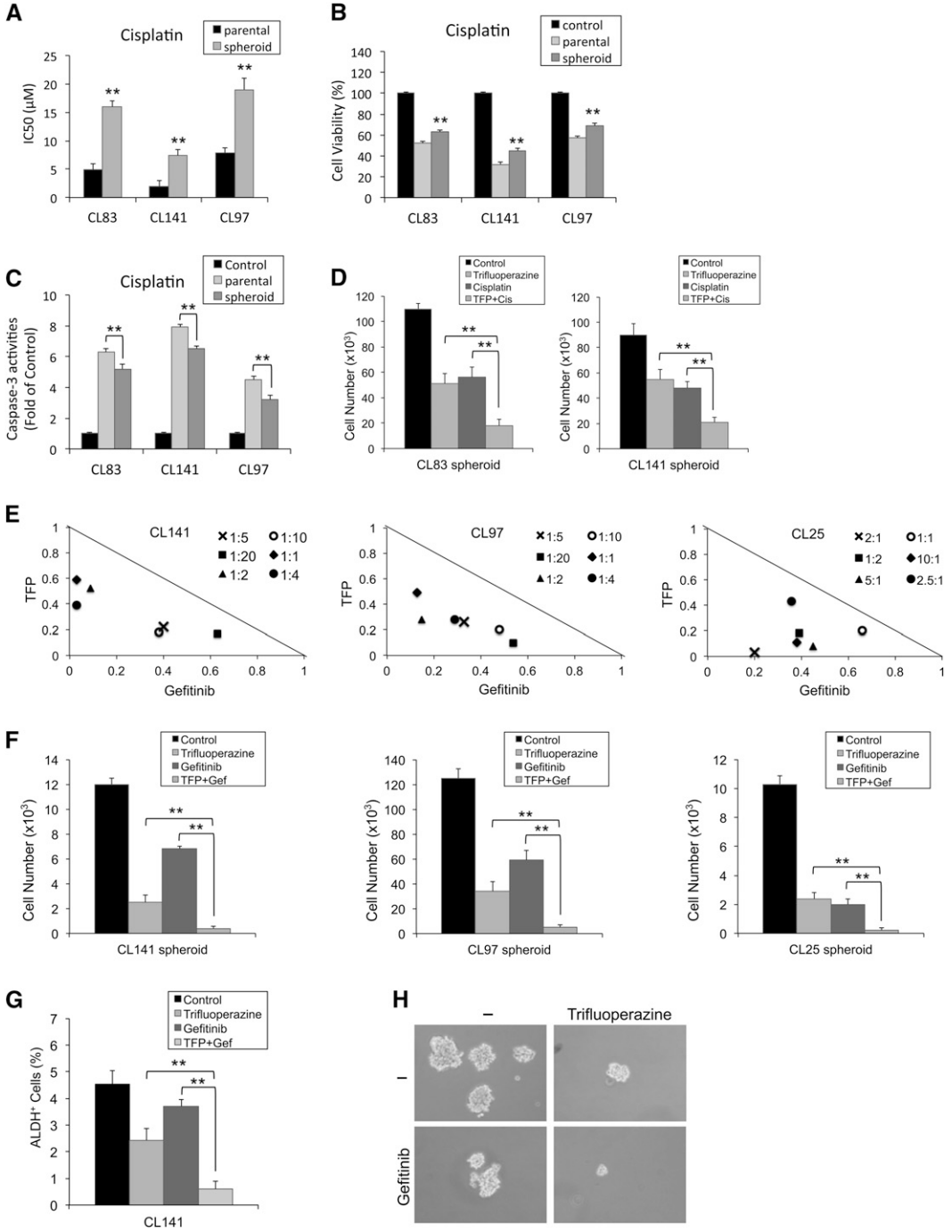

Figure 3. Trifluoperazine (TFP) effects in combination therapy and against tumor spheroids. (*A*) The half maximal inhibitory concentration of the conventional chemotherapy drug cisplatin on various non–small cell lung cancer spheroids and their corresponding parental cells. (*B* and *C*) Cell viability assay and caspase-3 activity assays for various non–small cell lung cancer spheroids treated with cisplatin (10 μM) for 24 hours. (*D*) CL83 and CL141 cancer spheroids were treated with TFP in combination with cisplatin, followed by cell number measurements. (*E*) Assessment of the combination of TFP and gefitinib by isobologram analysis. Normalized isobolograms for epidermal growth factor receptor wild-type (CL141) and epidermal growth factor receptor mutation cells (CL97 and CL25) exposed to all possible drug combinations of TFP (0.5, 2.5, and 5 μM), and gefitinib (2.5, 5, and 10 μM) for 48 hours. Symbols designate the combination index value for each fraction affected. The curves were generated by Calcusyn software to fit the experimental points. The data are representative of three independent experiments. Values below the line are synergistic, whereas those close to the line are additive and those above the line antagonistic. (*F*) CL141SP, CL97SP, and CL25SP were treated with TFP (10 μM), gefitinib (5 μM), or both, respectively, for 48 hours, followed by cell number measurement. (*G*) The aldehyde dehydrogenase $(ALDH)^+$ activity was analyzed in CL141 cells by flow cytometry, and the percentages of $ALDH^+$ cells are presented. (*H*) Disaggregated CL141 spheroids were seeded at clonal density on low-adhesion plates for secondary cancer spheroid formation. TFP enhanced gefitinib inhibition of CL141 self-renewal. *Columns* show mean of three independent experiments. *Bars* show SD. $^{**}P < 0.01$ as indicated.

EGFR-TKIs and chemotherapy. The combination of trifluoperazine and gefitinib led to reduced cell viability, ALDH-1 activity, and self-renewal of NSCLC spheroids. The combination of trifluoperazine and cisplatin also reduced cell viability and self-renewal of NSCLC spheroids, and enhanced caspase-3 activity. Notably, a recent report indicated that the canonical Wnt pathway protects lung cancer cells from EGFR inhibition and the disruption of Wnt/β-catenin signaling component enhances the efficacy of gefitinib (42). These results are in agreement with the observation that trifluoperazine-mediated suppression of β-catenin expression led to enhanced gefitnib efficacy. Eradicating CSCs to enhance treatment response and overcome drug resistance could become a common strategy for different cancer treatments in the future.

Trifluoperazine is a clinically approved drug, and thus the novel trifluoperazine combination therapy described herein could be fast-tracked into clinical trials. Clinical reports show that for advanced NSCLC, when cisplatin is combined with either with paclitaxel, docetaxel, or gemcitabine, an approximate 20% response rate and a median survival of less than 1 year was achieved (43). Thus, the combination of trifluoperazine with chemotherapeutic agents as a first-line therapy for advanced NSCLC may achieve a better treatment response and could prolong progression-free survival.

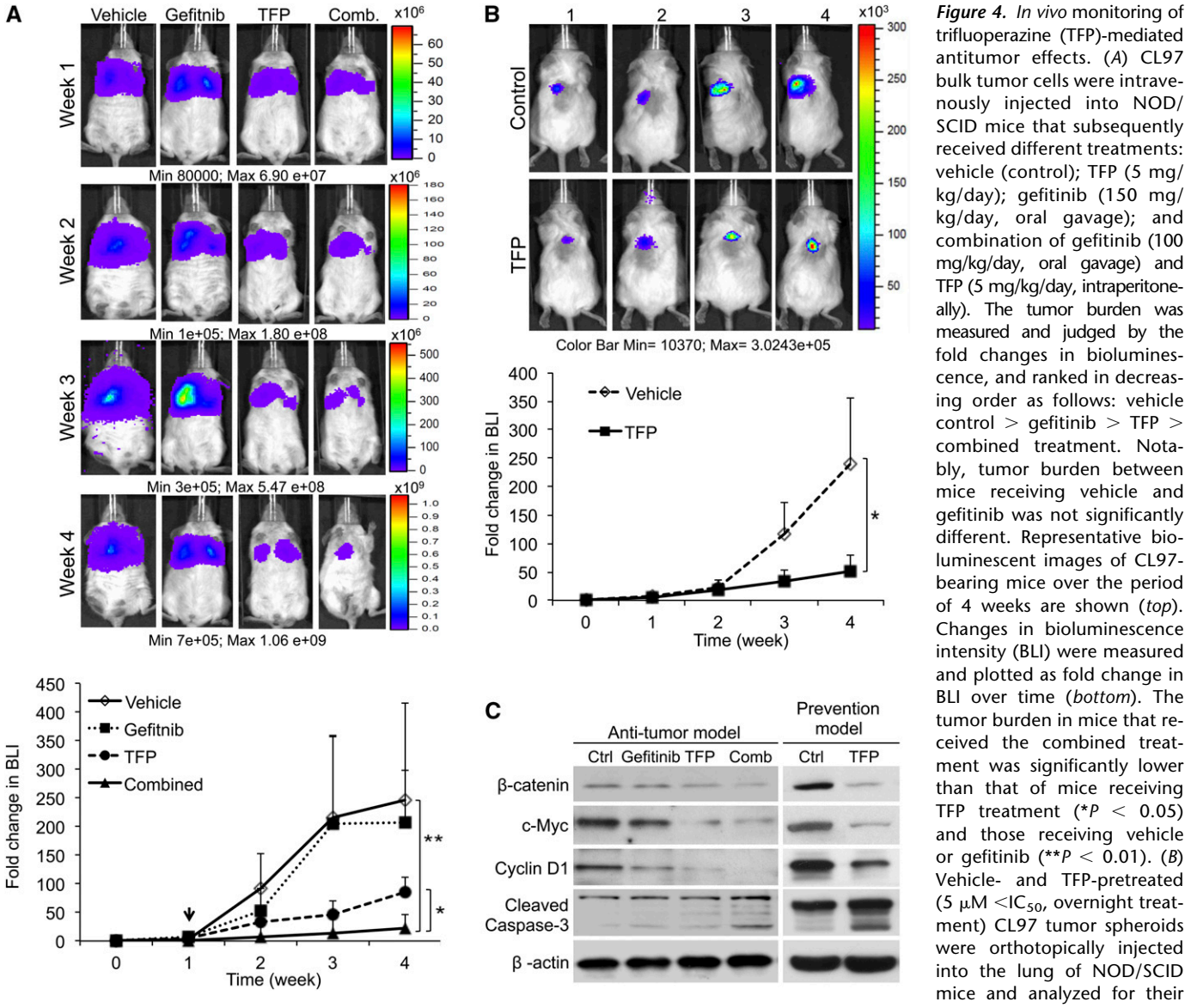

Figure 4. *In vivo* monitoring of trifluoperazine (TFP)-mediated antitumor effects. (*A*) CL97 bulk tumor cells were intravenously injected into NOD/SCID mice that subsequently received different treatments: vehicle (control); TFP (5 mg/kg/day); gefitinib (150 mg/kg/day, oral gavage); and combination of gefitinib (100 mg/kg/day, oral gavage) and TFP (5 mg/kg/day, intraperitoneally). The tumor burden was measured and judged by the fold changes in bioluminescence, and ranked in decreasing order as follows: vehicle control > gefitinib > TFP > combined treatment. Notably, tumor burden between mice receiving vehicle and gefitinib was not significantly different. Representative bioluminescent images of CL97-bearing mice over the period of 4 weeks are shown (*top*). Changes in bioluminescence intensity (BLI) were measured and plotted as fold change in BLI over time (*bottom*). The tumor burden in mice that received the combined treatment was significantly lower than that of mice receiving TFP treatment (*$P < 0.05$) and those receiving vehicle or gefitinib (**$P < 0.01$). (*B*) Vehicle- and TFP-pretreated (5 μM $<IC_{50}$, overnight treatment) CL97 tumor spheroids were orthotopically injected into the lung of NOD/SCID mice and analyzed for their tumorigenic ability. *In situ* tumor growth was significantly delayed and suppressed in TFP-pretreated animals, demonstrated by the representative bioluminescent images (*top*). Tumor growth was measured and plotted as fold change in BLI (*bottom*). The tumor burden was significantly different between the two groups (*$P < 0.05$). (*C*) Total cell lysates were harvested from tumor biopsies of mice that received different treatments and their protein profiles were examined. Samples from combined treatment demonstrated the most significant suppression of β-catenin, c-Myc, and cyclin D1 expression followed by TFP alone, gefitinib alone, and vehicle control. Proapoptotic molecule, caspase-3 expression level was increased in all treatment groups except for the vehicle control. Similarly, β-catenin, c-Myc, and cyclin D1 expression levels were suppressed in TFP-pretreated tumor spheroids, whereas activated caspase-3 expression was increased.

Gefitinib is effective for a subset of patients with particular mutations in the *EGFR* (e.g., L858R mutation), but ineffective to patients with wild-type *EGFR* or acquired mutation (T790M) (44). Almost all patients with lung adenocarcinoma with *EGFR* mutation eventually develop drug resistance after treatment with EGFR-TKIs. Based on our findings, the addition of trifluoperazine into the EGFR-TKI therapy may benefit patients with wild-type *EGFR* who do not have a satisfactory response to EGFR-TKI; the combination of trifluoperazine with EGFR-TKI may enhance the treatment response and improve therapeutic efficacy. More importantly, for patients harboring the *EGFR* mutation who develop gefitinib resistance, the addition of trifluoperazine may salvage therapy, extending the duration of gefitinib use and thereby prolonging progression-free survival.

In essence, we have identified trifluoperazine as an anti-CSC agent for NSCLC. Our findings demonstrate that trifluoperazine overcomes resistance to chemotherapy and EGFR-TKI *in vitro* and *in vivo*. Equally important, this study shows that the use of CMap in combination with a gene signature database of different diseases could serve as a high throughput platform for drug repurposing in the future.

Author disclosures are available with the text of this article at www.atsjournals.org.

Acknowledgment: The authors thank Po-Yang Huang for his technical support in animal imaging and tumor model establishments. The authors also thank Chun-Jung Lin (Cell Sorter Core Facility Center, Office of Research and Development, Taipei Medical University) for her assistance with the flow cytometry assay.

References

1. Siegel R, Naishadham D, Jemal A. Cancer statistics, 2012. *CA Cancer J Clin* 2012;62:10–29.
2. Pfister DG, Johnson DH, Azzoli CG, Sause W, Smith TJ, Baker S Jr, Olak J, Stover D, Strawn JR, Turrisi AT, *et al.* American Society of

Clinical Oncology treatment of unresectable non-small-cell lung cancer guideline: Update 2003. *J Clin Oncol* 2004;22:330–353.
3. Bao S, Wu Q, McLendon RE, Hao Y, Shi Q, Hjelmeland AB, Dewhirst MW, Bigner DD, Rich JN. Glioma stem cells promote radioresistance by preferential activation of the DNA damage response. *Nature* 2006; 444:756–760.
4. Diehn M, Cho RW, Lobo NA, Kalisky T, Dorie MJ, Kulp AN, Qian D, Lam JS, Ailles LE, Wong M, *et al.* Association of reactive oxygen species levels and radioresistance in cancer stem cells. *Nature* 2009;458:780–783.
5. Gupta PB, Onder TT, Jiang G, Tao K, Kuperwasser C, Weinberg RA, Lander ES. Identification of selective inhibitors of cancer stem cells by high-throughput screening. *Cell* 2009;138:645–659.
6. Clevers H. The cancer stem cell: premises, promises and challenges. *Nat Med* 2011;17:313–319.
7. Eramo A, Lotti F, Sette G, Pilozzi E, Biffoni M, Di Virgilio A, Conticello C, Ruco L, Peschle C, De Maria R. Identification and expansion of the tumorigenic lung cancer stem cell population. *Cell Death Differ* 2008;15: 504–514.
8. Pirozzi G, Tirino V, Camerlingo R, Franco R, La Rocca A, Liguori E, Martucci N, Paino F, Normanno N, Rocco G. Epithelial to mesenchymal transition by TGF beta-1 induction increases stemness characteristics in primary non small cell lung cancer cell line. *PLoS ONE* 2011;6: e21548.
9. Leung EL, Fiscus RR, Tung JW, Tin VP, Cheng LC, Sihoe AD, Fink LM, Ma Y, Wong MP. Non-small cell lung cancer cells expressing CD44 are enriched for stem cell-like properties. *PLoS ONE* 2010;5:e14062.
10. Storms RW, Goodell MA, Fisher A, Mulligan RC, Smith C. Hoechst dye efflux reveals a novel CD7(+)CD34(-) lymphoid progenitor in human umbilical cord blood. *Blood* 2000;96:2125–2133.
11. Ginestier C, Hur MH, Charafe-Jauffret E, Monville F, Dutcher J, Brown M, Jacquemier J, Viens P, Kleer CG, Liu S, *et al.* ALDH1 is a marker of normal and malignant human mammary stem cells and a predictor of poor clinical outcome. *Cell Stem Cell* 2007;1:555–567.
12. Ozvegy-Laczka C, Hegedus T, Varady G, Ujhelly O, Schuetz JD, Varadi A, Keri G, Orfi L, Nemet K, Sarkadi B. High-affinity interaction of tyrosine kinase inhibitors with the ABCG2 multidrug transporter. *Mol Pharmacol* 2004;65:1485–1495.
13. Shats I, Gatza ML, Chang JT, Mori S, Wang J, Rich J, Nevins JR. Using a stem cell-based signature to guide therapeutic selection in cancer. *Cancer Res* 2011;71:1772–1780.
14. Wong DJ, Liu H, Ridky TW, Cassarino D, Segal E, Chang HY. Module map of stem cell genes guides creation of epithelial cancer stem cells. *Cell Stem Cell* 2008;2:333–344.
15. Kim J, Woo AJ, Chu J, Snow JW, Fujiwara Y, Kim CG, Cantor AB, Orkin SH. A Myc network accounts for similarities between embryonic stem and cancer cell transcription programs. *Cell* 2010;143:313–324.
16. Lamb J, Crawford ED, Peck D, Modell JW, Blat IC, Wrobel MJ, Lerner J, Brunet JP, Subramanian A, Ross KN, *et al.* The connectivity map: using gene-expression signatures to connect small molecules, genes, and disease. *Science* 2006;313:1929–1935.
17. Zufferey R, Nagy D, Mandel RJ, Naldini L, Trono D. Multiply attenuated lentiviral vector achieves efficient gene delivery in vivo. *Nat Biotechnol* 1997;15:871–875.
18. Chou TC, Talalay P. Quantitative analysis of dose-effect relationships: the combined effects of multiple drugs or enzyme inhibitors. *Adv Enzyme Regul* 1984;22:27–55.
19. Engelman JA, Zejnullahu K, Gale CM, Lifshits E, Gonzales AJ, Shimamura T, Zhao F, Vincent PW, Naumov GN, Bradner JE, *et al.* Pf00299804, an irreversible pan-ERBB inhibitor, is effective in lung cancer models with EGFR and ERBB2 mutations that are resistant to gefitinib. *Cancer Res* 2007;67:11924–11932.
20. Yan Y, Lu Y, Wang M, Vikis H, Yao R, Wang Y, Lubet RA, You M. Effect of an epidermal growth factor receptor inhibitor in mouse models of lung cancer. *Mol Cancer Res* 2006;4:971–981.
21. Liu H, Patel MR, Prescher JA, Patsialou A, Qian D, Lin J, Wen S, Chang YF, Bachmann MH, Shimono Y, *et al.* Cancer stem cells from human breast tumors are involved in spontaneous metastases in orthotopic mouse models. *Proc Natl Acad Sci USA* 2010;107:18115–18120.
22. Zhang M, Rosen JM. Stem cells in the etiology and treatment of cancer. *Curr Opin Genet Dev* 2006;16:60–64.
23. Ben-Porath I, Thomson MW, Carey VJ, Ge R, Bell GW, Regev A, Weinberg RA. An embryonic stem cell-like gene expression signature in poorly differentiated aggressive human tumors. *Nat Genet* 2008;40: 499–507.
24. Somervaille TC, Matheny CJ, Spencer GJ, Iwasaki M, Rinn JL, Witten DM, Chang HY, Shurtleff SA, Downing JR, Cleary ML. Hierarchical maintenance of MLL myeloid leukemia stem cells employs a transcriptional program shared with embryonic rather than adult stem cells. *Cell Stem Cell* 2009;4:129–140.
25. Ramalho-Santos M, Yoon S, Matsuzaki Y, Mulligan RC, Melton DA. Stemness: transcriptional profiling of embryonic and adult stem cells. *Science* 2002;298:597–600.
26. Suva ML, Riggi N, Janiszewska M, Radovanovic I, Provero P, Stehle JC, Baumer K, Le Bitoux MA, Marino D, Cironi L, *et al.* EZH2 is essential for glioblastoma cancer stem cell maintenance. *Cancer Res* 2009;69:9211–9218.
27. Sachlos E, Risueno RM, Laronde S, Shapovalova Z, Lee JH, Russell J, Malig M, McNicol JD, Fiebig-Comyn A, Graham M, *et al.* Identification of drugs including a dopamine receptor antagonist that selectively target cancer stem cells. *Cell* 2012;149:1284–1297.
28. Paul S, Dey A. Wnt signaling and cancer development: therapeutic implication. *Neoplasma* 2008;55:165–176.
29. Nguyen DX, Chiang AC, Zhang XH, Kim JY, Kris MG, Ladanyi M, Gerald WL, Massague J. WNT/TCF signaling through LEF1 and HOXB9 mediates lung adenocarcinoma metastasis. *Cell* 2009;138:51–62.
30. Mazieres J, He B, You L, Xu Z, Jablons DM. Wnt signaling in lung cancer. *Cancer Lett* 2005;222:1–10.
31. Seeman P, Lee T, Chau-Wong M, Wong K. Antipsychotic drug doses and neuroleptic/dopamine receptors. *Nature* 1976;261:717–719.
32. Marques LO, Lima MS, Soares BG. Trifluoperazine for schizophrenia. *Cochrane Database Syst Rev* 2004;CD003545.
33. Vandonselaar M, Hickie RA, Quail JW, Delbaere LT. Trifluoperazine-induced conformational change in Ca(2+)-calmodulin. *Nat Struct Biol* 1994;1:795–801.
34. Pan D, Yan Q, Chen Y, McDonald JM, Song Y. Trifluoperazine regulation of calmodulin binding to Fas: a computational study. *Proteins* 2011;79:2543–2556.
35. Chen QY, Wu LJ, Wu YQ, Lu GH, Jiang ZY, Zhan JW, Jie Y, Zhou JY. Molecular mechanism of trifluoperazine induces apoptosis in human A549 lung adenocarcinoma cell lines. *Mol Med Report* 2009;2:811–817.
36. Shin SY, Choi BH, Kim JR, Kim JH, Lee YH. Suppression of P-glycoprotein expression by antipsychotics trifluoperazine in adriamycin-resistant l1210 mouse leukemia cells. *Eur J Pharm Sci* 2006;28:300–306.
37. Shin SY, Kim CG, Hong DD, Kim JH, Lee YH. Implication of Egr-1 in trifluoperazine-induced growth inhibition in human U87MG glioma cells. *Exp Mol Med* 2004;36:380–386.
38. Hendrich AB, Wesolowska O, Michalak K. Trifluoperazine induces domain formation in zwitterionic phosphatidylcholine but not in charged phosphatidylglycerol bilayers. *Biochim Biophys Acta* 2001; 1510:414–425.
39. Ford JM, Prozialeck WC, Hait WN. Structural features determining activity of phenothiazines and related drugs for inhibition of cell growth and reversal of multidrug resistance. *Mol Pharmacol* 1989;35:105–115.
40. Ganapathi R, Kuo T, Teeter L, Grabowski D, Ford J. Relationship between expression of P-glycoprotein and efficacy of trifluoperazine in multidrug-resistant cells. *Mol Pharmacol* 1991;39:1–8.
41. Hanahan D, Weinberg RA. Hallmarks of cancer: the next generation. *Cell* 2011;144:646–674.
42. Casas-Selves M, Kim J, Zhang Z, Helfrich BA, Gao D, Porter CC, Scarborough HA, Bunn PA Jr, Chan DC, Tan AC, *et al.* Tankyrase and the canonical Wnt pathway protect lung cancer cells from EGFR inhibition. *Cancer Res* 2012;72:4154–4164.
43. Schiller JH, Harrington D, Belani CP, Langer C, Sandler A, Krook J, Zhu J, Johnson DH. Comparison of four chemotherapy regimens for advanced non-small-cell lung cancer. *N Engl J Med* 2002;346:92–98.
44. Mok TS, Wu YL, Thongprasert S, Yang CH, Chu DT, Saijo N, Sunpaweravong P, Han B, Margono B, Ichinose Y, *et al.* Gefitinib or carboplatin-paclitaxel in pulmonary adenocarcinoma. *N Engl J Med* 2009;361:947–957.